

AN *XMM-NEWTON* OBSERVATION OF THE HIGH MAGNETIC FIELD RADIO PULSAR PSR B0154+61

M. E. GONZALEZ,^{1,2} V. M. KASPI,^{1,3} A. G. LYNE,⁴ AND M. J. PIVOVAROFF⁵

Received 2004 May 4; accepted 2004 June 4; published 2004 June 14

ABSTRACT

We present the results obtained from a 31 ks *XMM-Newton* observation of the high magnetic field radio pulsar PSR B0154+61. This relatively nearby pulsar has an inferred dipole surface magnetic field strength of 2.1×10^{13} G, among the highest in the population. This makes the pulsar a possible transition object between the classical radio pulsars and magnetars, whose enhanced X-ray emission is believed to be powered by their large magnetic fields. However, our analysis shows that no X-ray emission is detected from the position of PSR B0154+61 with *XMM-Newton*. The upper flux limit derived from the observation implies a blackbody temperature of $T_{\text{bb}}^{\infty} \lesssim 73$ eV and unabsorbed 0.3–10.0 keV X-ray luminosity of $\lesssim 1.4 \times 10^{32}$ ergs s^{-1} (assuming a distance of 2.2 kpc and column density of $N_{\text{H}} \lesssim 3 \times 10^{21}$ cm^{-2}). This luminosity is much lower than those exhibited by all known magnetars. When corrections for the presence of a light-element atmosphere on the neutron star are made, our estimates favor the temperature predictions of rapid cooling models over those of standard cooling models. However, the uncertainties in distance, column density, and atmospheric composition prevent a definite conclusion regarding initial cooling.

Subject headings: pulsars: general — pulsars: individual (PSR B0154+61) — X-rays: general

1. INTRODUCTION

The past two decades saw a new class of X-ray pulsars (PSRs) emerge that does not appear to be powered by the common rotation or accretion mechanisms (Mereghetti & Stella 1995). These “anomalous” X-ray pulsars (AXPs) are characterized by their long periods (~ 6 – 12 s), absence of radio emission, X-ray luminosity several orders of magnitude higher than their spin-down luminosity, and high inferred surface magnetic field strengths ($\sim 10^{14}$ – 10^{15} G). These properties are similar to those exhibited by soft gamma repeaters (SGRs). A close, and possibly evolutionary, relationship between these two classes of objects has recently been demonstrated (Gavriil et al. 2002; Kaspi et al. 2003). To date, the most favored model put forward to explain the characteristics of these objects is the “magnetar” model (Thompson & Duncan 1995). Here, magnetic field decay from the stellar interior heats up the star and results in the observed X-ray luminosities.

On the other hand, the X-ray emission of rotation-powered neutron stars (NSs) is believed to arise mainly from three regions—the magnetosphere and surface and polar caps (see, e.g., Pavlov et al. 2002; Kaspi et al. 2004). In particular, the surface emission arises from processes taking place deep within the stars. In young NSs ($\lesssim 10^5$ yr) cooling through neutrino emission from the interior, the surface emission follows the thermal evolution of the core and is modified as it passes through the outer stellar envelope. In older stars ($\gtrsim 10^5$ yr) cooling through photon emission, the neutrino production mechanism becomes inefficient and the thermal radiation from the surface governs the energy loss from the interior. The “standard” cooling predictions of NSs involve slow processes such as the modified Urca, plasmon neutrino, and bremsstrahlung mechanisms. The “fast” cooling predictions involve more ex-

otic, efficient processes such as direct Urca and possibly hyperons, pions, kaons, and quarks (see Yakovlev & Pethick 2004 for a review). Therefore, observing the cooling radiation from these NSs offers the opportunity of constraining the structure of matter at supranuclear densities. In addition, this emission can provide insights into basic properties of the stellar surface, such as its temperature, composition, and effective emitting area.

In order to test the above models of NS evolution, a broad sample of interesting sources must be studied. One such source is PSR B0154+61. It has a period $P = 2.35$ s, period derivative $\dot{P} = 1.89 \times 10^{-13}$, characteristic age $\tau_c = 197$ kyr, spin-down luminosity $\dot{E} = 5.7 \times 10^{32}$ ergs s^{-1} , and inferred dipole surface magnetic field strength $B = 2.1 \times 10^{13}$ G (Arzoumanian et al. 1994). The pulsar’s rotation period and inferred magnetic field are among the highest in the radio pulsar population and close to those exhibited by magnetars. In addition, the intermediate age and low spin-down luminosity of PSR B0154+61 argue for thermal emission to still be present and to dominate over nonthermal magnetospheric or nebular emission. From the dispersion measure (DM) and a model of the free electron distribution in the Galaxy, the pulsar lies at a close distance of ~ 1.7 kpc (Cordes & Lazio 2002), increasing the chance of detecting thermal emission from the NS surface. In this Letter, we present the analysis of an *XMM-Newton* observation of the pulsar and compare our results to those expected from magnetars and cooling neutron stars.

2. OBSERVATION AND DATA ANALYSIS

PSR B0154+61 was observed with *XMM-Newton* on 2003 March 6. The European Photon Imaging Camera (EPIC) instruments MOS (Turner et al. 2001) and PN (Strüder et al. 2001) were operated in full-window (imaging) and small-window modes, respectively. These settings provide a temporal resolution of 1.4 s for MOS and 6 ms for PN. The medium filters were used for MOS, while the thin filter was used on the PN. The Optical Monitor (OM) instrument was operated in image mode, and an observation with the Resolution Grating Spectrometer (RGS) was also obtained.

The EPIC data were reduced with the *XMM-Newton* Science

¹ Department of Physics, McGill University, Rutherford Physics Building, 3600 University Street, Montreal QC H3A 2T8, Canada.

² NSERC PGS-B (Ph.D.); gonzalez@physics.mcgill.ca.

³ Canada Research Chair, Steacie Fellow.

⁴ Jodrell Bank Observatory, University of Manchester, Macclesfield, Cheshire SK11 9DL, UK.

⁵ Lawrence Livermore National Laboratory, University of California, P.O. Box 808, L-413, Livermore, CA 94550.

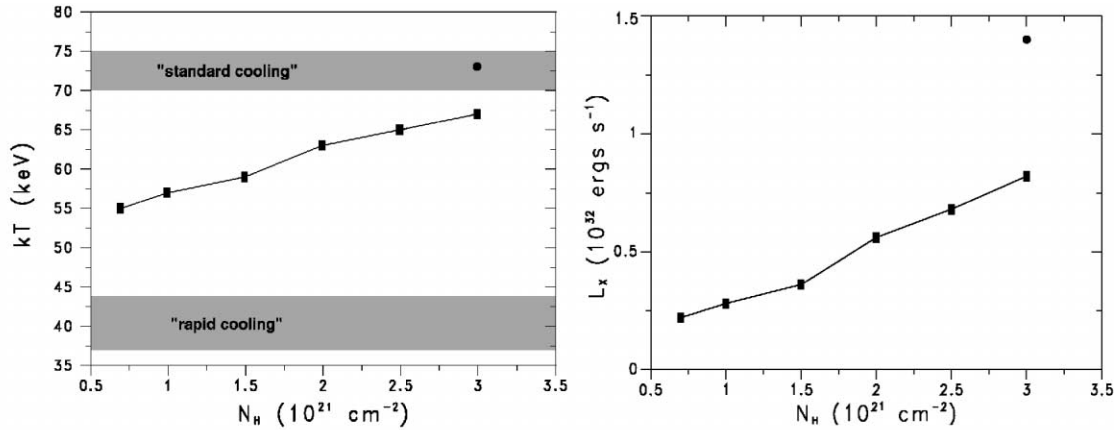


FIG. 1.—Upper limits derived from the blackbody surface temperature (*left*) and unabsorbed 0.3–10.0 keV luminosity (*right*) of PSR B0154+61 with *XMM-Newton*. The squares represent limits derived assuming the DM distance of 1.7 kpc, and the circles represent limits at a distance of 2.2 kpc (see § 3). The predicted temperature ranges from “standard” and “rapid” cooling models are also shown (see § 4).

Analysis System (SAS ver. 5.4.1). In order to maximize the signal-to-noise ratio (S/N), the data were filtered to include single, double, triple, and quadruple pixel events for MOS and single and double pixel events for PN. Light curves from source-free regions in these detectors were examined, and no significant background changes or flares were found. The resulting exposure time for the two MOS detectors was ~ 31 ks. For PN, only $\sim 70\%$ of the live time was used in the small-window mode, resulting in an exposure time of ~ 22 ks.

Individual images for a soft (0.3–2.0 keV) and a hard (2.0–15.0 keV) X-ray band were first obtained, binning the original MOS pixels into $2''5 \times 2''5$ pixels. Following the procedure outlined by the *XMM-Newton* Science Operation Center,⁶ the SAS source detection algorithms *evselect* and *eboxselect* were applied to the data. As suggested from visual inspection, no X-ray counterpart for PSR B0154+61 was found in the MOS1 data down to the $S/N \sim 2.5 \sigma$ level. The closest source to the radio coordinates is located $\sim 45''$ away and was only detected with a $S/N \sim 3$. The same result was obtained when analyzing the MOS2 and PN data with the above algorithms. In addition, a quick inspection of the RGS and OM data reveal similar conclusions.

3. RESULTS

Although no direct emission was detected from PSR B0154+61, we can derive upper limit estimates for its detection, which can then be compared to current predictions. To increase our sensitivity, the following results are derived using the combined MOS1 and MOS2 count rates. The simulated spectral models were folded through the response matrices of the MOS1 detector, with identical results obtained if using MOS2.

In order to calculate an upper limit on the count rate, we compare the counts collected from an aperture of radius $15''$ centered on the radio coordinates of the pulsar with those of a concentric annulus with radii $15''$ – $20''$. Following the method described by Pivovarov et al. (2000), a detection at the $S/N > 3 \sigma$ level requires an upper limit in the 0.3–10.0 keV band of $\leq 1.3 \times 10^{-3}$ counts s^{-1} . We can then use this upper limit on the count rate to estimate an upper limit on parameters such as the NS’s surface temperature and luminosity. In turn,

these values can be compared to those observed for other objects, such as AXPs, and the values predicted from NS cooling models.

A simple estimate for the temperature and luminosity at the pulsar’s surface can be made by assuming a blackbody spectrum modified by interstellar absorption. The model *bbbodyrad*, available with XSPEC version 11.1.0, was then used. The model depends on the surface temperature kT (in units of keV) and emission measure of the source. Here, the emission measure is given by R_{km}^2/D_{10}^2 , where R_{km} is the NS’s radius (in kilometers) and D_{10} is the distance (in units of 10 kpc). In our simulations, we use the canonical value for the NS radius of 10 km and, as a first try, a distance of 1.7 kpc as suggested by the pulsar’s DM. Holding these parameters fixed for each run (as well as the interstellar absorption; see below) allows us to fit for the NS temperature needed to reproduce the upper limit on the count rate.

Furthermore, an estimate for the amount of interstellar absorption (N_H) in the direction of the pulsar is needed. A first approximation can be made by assuming ~ 10 neutral hydrogen atoms for each free electron, giving a value of $N_H \sim 1 \times 10^{21} \text{ cm}^{-2}$. A more valid approximation is possible by using a set of reference interstellar medium column densities close to the pulsar’s location in the Galaxy. Such reference data are available through the *Extreme Ultraviolet Explorer* (*EUVE*) data analysis tools.⁷ For the 10 closest sources to the pulsar in space that are listed, at distances from the Earth of 1.1–2.3 kpc, the reference data find an average absorption of $N_H \sim 2 \times 10^{21} \text{ cm}^{-2}$, with a range of $\sim (0.7$ – $3.0) \times 10^{21} \text{ cm}^{-2}$. In addition, the total galactic column density⁸ in the direction of the pulsar is $\sim 9.5 \times 10^{21}$. The *EUVE* estimates are then reasonable given the pulsar’s close distance; they also agree with our first approximation and are therefore used in the following calculations.

At the DM distance of 1.7 kpc and assuming an average absorption of $N_H \sim 2 \times 10^{21} \text{ cm}^{-2}$, the upper count rate limit estimation results in an effective blackbody surface temperature of $T_{\text{bb,eff}}^\infty \leq 63$ eV and unabsorbed X-ray luminosity in the 0.3–10.0 keV band of $L_x \leq 0.6 \times 10^{32} D_{1.7}^2 \text{ ergs s}^{-1}$, where $D_{1.7}$ is the distance in units of 1.7 kpc. Taking the full range of N_H values from above into account, we get $T_{\text{bb,eff}}^\infty \leq 55$ – 67 eV and $L_x \leq (0.2$ – $0.8) \times 10^{32} D_{1.7}^2 \text{ ergs s}^{-1}$. Figure 1 shows a plot of

⁶ See http://xmm.vilspa.esa.es/external/xmm_sw_cal/sas_frame.shtml.

⁷ See <http://archive.stsci.edu/euve/ism/ismform.html>.

⁸ See <http://heasarc.gsfc.nasa.gov/cgi-bin/Tools/w3nh/w3nh.pl>.

TABLE 1
COMPARISON OF HIGH MAGNETIC FIELD RADIO PULSARS WITH AXPs

| Name | P (s) | τ_c (kyr) | B (10^{13} G) | \dot{E} (ergs s^{-1}) | L_x (ergs s^{-1}) |
|----------------------|------------|-------------------|-----------------------|-------------------------------|-----------------------------|
| AXPs: | | | | | |
| 1E 1841–045 | 11.8 | 4.5 | 71 | 9.9×10^{32} | 2.3×10^{35} |
| 1E 1048.1–5937 | 6.45 | ~ 2.7 | ~ 50 | $\sim 55 \times 10^{32}$ | 3.4×10^{34} |
| RXS J1708–4009 | 11.0 | 9.4 | 46 | 5.4×10^{32} | 6.8×10^{35} |
| 4U 0142+61 | 8.69 | 7.0 | 13 | 1.2×10^{32} | 3.3×10^{34} |
| 1E 2259+586 | 6.98 | 230 | 5.9 | 0.55×10^{32} | 1.0×10^{35} |
| Radio pulsars: | | | | | |
| J1847–0130 | 6.7 | 83 | 9.4 | 1.7×10^{32} | $<(3-8) \times 10^{33}$ |
| J1814–1744 | 4.0 | 85 | 5.5 | 4.7×10^{32} | $<4.3 \times 10^{33}$ |
| J1119–6127 | 0.407 | 1.6 | 4.1 | 2.3×10^{36} | $\sim(2-16) \times 10^{32}$ |
| B0154+61 | 2.35 | 197 | 2.1 | 5.7×10^{32} | $<1.4 \times 10^{32}$ |

these values; the shaded regions represent the temperature predictions from NS cooling models (see below). In addition, allowing for a conservative error in the DM distance of 30%, the upper limits at the highest estimated N_H -value are $\lesssim 73$ eV and $\lesssim 1.4 \times 10^{32} D_{2.2}^2$ ergs s^{-1} for the temperature and unabsorbed 0.3–10.0 keV luminosity, respectively ($D_{2.2}$ is the distance in units of 2.2 kpc). It is also worth noting that individual pulsar distances measured from other techniques can vary significantly from the DM distance (sometimes by a factor of ~ 3 ; e.g., Brisken et al. 2003). Such a high discrepancy in the distance to PSR B0154+61 would greatly affect our results. An independent determination of the distance would therefore improve our understanding of this object.

4. DISCUSSION

4.1. Implications for Magnetar Models

PSR B0154+61 is one of a few pulsars that exhibit spin characteristics similar to those of SGRs and AXPs. However, given our luminosity upper limits, its X-ray emission is apparently very different from these objects.

As discussed in § 1, emission from high-magnetic field sources such as AXPs/SGRs has been explained by the magnetar model. Here, their X-ray and gamma-ray luminosities are attributed to the decay of their ultrastrong magnetic field. The properties for these objects can be well explained using this model, which also allows for an evolutionary link to be made between the two classes of objects. However, the remaining challenge is to find the missing link between radio pulsars and magnetars.

On this effort, several high magnetic field radio pulsars have now been observed at X-ray wavelengths (see Pivovarov et al. 2000; Gonzalez & Safi-Harb 2003; McLaughlin et al. 2003). Table 1 compares the properties of these pulsars with those of AXPs (Kaspi & Gavriil 2004) and illustrates that the high-energy emission mechanisms of these objects must be greatly different. These radio pulsars have dipole magnetic fields in the range $B \sim 10^{13}$ – 10^{14} G. This is a regime that, if AXP/SGR-like behavior depends exclusively on the inferred value of the magnetic field, should yield similar X-ray luminosities for these objects, contrary to what is observed.

We can then wonder about the reasons for this discrepancy. First, given the overlap between the inferred fields listed in Table 1, the possibility that the magnetar mechanism turns on above a critical field does not seem likely (see below). In addition, the magnetic field alone might not determine whether a source will exhibit magnetar-like behavior. However, the fact that other properties are not well constrained (such as mass, radius, composition, environment, etc.) makes this option hard

to evaluate at the present. Another possibility is that the inferred fields are not representative of the true fields in these objects. They could be close to the dipole component values. However, further contributions to the spin-down would go undetected if present, for example, in the form of higher order multiple components or external torque contributions (e.g., Alpar et al. 2001), although there is no observational evidence for this at the present. In addition, it is also worth noting that for deviations from pure dipole fields, the presence of a critical field for the onset of magnetar-like behavior could not be ruled out from the values listed in Table 1.

Various additional models have been proposed to explain the observed differences between high B -field radio pulsars and magnetars (see, e.g., McLaughlin et al. 2003, and references therein). However, until a clear link between these objects is found (in the form of radio emission from an AXP/SGR or magnetar-like emission from a high B -field radio pulsar), the physical nature of their similarities and differences will remain a mystery.

4.2. Implications for Cooling Models

The above temperature estimates can also be compared to those predicted from NS cooling models. However, the effects of an atmosphere and high magnetic field must first be taken into account.

The spectrum from an NS atmosphere can be very different from a blackbody. A light-element atmosphere (such as H or He) will have an apparently harder X-ray spectrum than a blackbody at the same effective temperature (see, e.g., Zavlin & Pavlov 2002; Lloyd et al. 2003). Therefore, these atmospheres have temperatures T_{atm} significantly lower than that measured using a blackbody T_{bb} , with ratios usually on the order of $T_{\text{bb}}/T_{\text{atm}} \sim 1.5$ – 3 (e.g., McGowan et al. 2003; Pavlov et al. 2002). However, in order to provide the same bolometric flux, a light-element atmosphere gives a larger size for the emitting region or, conversely, a distance that is too small. On the other hand, heavy-element atmospheres (such as Fe) have overall high-opacity trends that produce spectra much closer to a blackbody than light-element atmospheres, and in some cases with $T_{\text{bb}}/T_{\text{atm}} \lesssim 1$ (see, e.g., Rajagopal et al. 1997). In addition, magnetized atmosphere models with either light or heavy elements have shown that a high magnetic field ($B \gtrsim 10^{13}$ G) will increase opacities and produce emergent spectra closer to a blackbody. In this case, light-element atmospheres still produce a further deviation from a blackbody than heavy-element atmospheres (see, e.g., Lloyd et al. 2003; Ho & Lai 2001; Rajagopal et al. 1997).

Therefore, our derived upper limit values for the surface tem-

perature of B0154+61 would decrease in the presence of a light-element atmosphere on the NS. For a ratio of $T_{\text{bb}}/T_{\text{atm}} \sim 1.5$ (on the low end of the observed and predicted values, including magnetized atmospheres), our highest surface temperature estimate of $T_{\text{bb}} \lesssim 73$ eV would imply $T_{\text{atm}} \lesssim 49$ eV. However, the presence of a heavy-element atmosphere would support our original value or even raise it.

For a characteristic age of $\tau_c = 197$ kyr as derived for PSR B0154+61,⁹ standard cooling models predict an NS surface temperature of $T_{\text{std}} \sim 70\text{--}75$ eV, while rapid cooling models predict $T_{\text{rapid}} \sim 37\text{--}44$ eV (see Fig. 1 and, e.g., Page 1998). Unfortunately, at the above age the pulsar is located close to the transition stage between the neutrino and the photon cooling eras (see § 1), where predictions are very sensitive to the specific model parameters. Consequently, different results are produced from various models accounting for the atmospheric composition and magnetic field of the star. For example, simplified models at high B -fields by Page (1995) and Shibano & Yakovlev (1996) produce little difference in the predicted temperatures for standard cooling models, with the temperatures for

⁹ This age is probably not an overestimate, as a birth spin period $P_0 \ll P$ is likely for this long-period pulsar. However, an underestimate of τ_c by a factor of greater than 10 would imply a braking index $n < 1.2$ (comparable to that estimated for the Vela pulsar; Lyne et al. 1996), which cannot be ruled out and would have major implications for the evolution of the pulsar population as a whole.

the rapid cooling models increasing to $T_{\text{rapid}} \sim 42\text{--}51$ eV (at most) at $B = 10^{13}$ G. On the other hand, for the same magnetic field, the atmospheric models of Potekhin et al. (2003) predict surface temperatures of $T_{\text{std}} \sim 60\text{--}65$ eV and $T_{\text{rapid}} \lesssim 13$ eV (the lower limits corresponding to heavy-element atmospheres).

From the above results, the agreement of our surface temperature upper limit with cooling predictions depends on the specific characteristics of the NS, and more strongly on the atmospheric composition than magnetic field value. If a light-element atmosphere is present, our blackbody upper limit would be lowered to $T_{\text{atm}} \lesssim 49$ eV, in agreement only with the predicted values from rapid cooling models. However, a heavy-element atmosphere would imply an upper limit of $T_{\text{atm}} \lesssim 73$ eV (and maybe higher), in closer agreement to the values predicted from standard cooling models. At present, light-element atmospheres are somewhat favored over heavy-element atmospheres from high-resolution X-ray spectra of numerous NSs (see Pavlov et al. 2002 for a review). In this case, rapid cooling models would then be favored for PSR B0154+61. However, problems with light-element atmosphere predictions, such as a large emitting area and higher than observed optical fluxes, call for more studies to be made.

This work was supported in part by an NSERC Discovery Grant and Steacie Supplement, FCAR/NATEQ grants, a Canadian Institute for Advanced Research Fellowship, the Canada Research Chair Program, and NASA/LTSA.

REFERENCES

- Alpar, M. A., Ankay, A., & Yazgan, E. 2001, *ApJ*, 557, L61
 Arzoumanian, Z., Nice, D. J., Taylor, J. H., & Thorsett, S. E. 1994, *ApJ*, 422, 671
 Brisken, W. F., Thorsett, S. E., Golden, A., & Goss, W. M. 2003, *ApJ*, 593, L89
 Cordes, J. M., & Lazio, T. J. W. 2002, preprint (astro-ph/0207156)
 Gavriil, F. P., Kaspi, V. M., & Woods, P. M. 2002, *Nature*, 419, 142
 Gonzalez, M., & Safi-Harb, S. 2003, *ApJ*, 591, L143
 Ho, W. C. G., & Lai, D. 2001, *MNRAS*, 327, 1081
 Kaspi, V. M., & Gavriil, F. P. 2004, in *The Restless High-Energy Universe*, ed. E. P. J. van den Heuvel, J. J. M. in 't Zand, & R. A. M. J. Wijers, in press (astro-ph/0402176)
 Kaspi, V. M., Gavriil, F. P., Woods, P. M., Jensen, J. B., Roberts, M. S. E., & Chakrabarty, D. 2003, *ApJ*, 588, L93
 Kaspi, V. M., Roberts, M. S. E., & Harding, A. K. 2004, in *Compact Stellar X-Ray Sources*, ed. W. H. G. Lewin & M. van der Klis, in press (astro-ph/0402136)
 Lloyd, D. A., Hernquist, L., & Heyl, J. S. 2003, *ApJ*, 593, 1024
 Lyne, A. G., Pritchard, R. S., Graham-Smith, F., & Camilo, F. 1996, *Nature*, 381, 497
 McGowan, K. E., et al. 2003, *ApJ*, 591, 380
 McLaughlin, M. A., et al. 2003, *ApJ*, 591, L135
 Mereghetti, S., & Stella, L. 1995, *ApJ*, 442, L17
 Page, D. 1995, *ApJ*, 442, 273
 ———. 1998, in *The Many Faces of Neutron Stars*, ed. R. Buccheri, J. van Paradijs, & M. A. Alpar (Dordrecht: Kluwer), 539
 Pavlov, G. G., Zavlin, V. E., & Sanwal, D. 2002, in *Proc. 270 WE-Heraeus Seminar on Neutron Stars, Pulsars, and Supernova Remnants*, ed. W. Becker, H. Lesch, & J. Trümper (MPE Rep. 278; Garching: MPE), 273
 Pivovarov, J. M., Kaspi, V. M., & Camilo, F. 2000, *ApJ*, 535, 379
 Potekhin, A. Y., Yakovlev, D. G., Chabrier, G., & Gnedin, O. Y. 2003, *ApJ*, 594, 404
 Rajagopal, M., Romani, R. W., & Miller, M. C. 1997, *ApJ*, 479, 347
 Shibano, Y. A., & Yakovlev, D. G. 1996, *A&A*, 309, 171
 Strüder, L., et al. 2001, *A&A*, 365, L18
 Thompson, C., & Duncan, R. C. 1995, *MNRAS*, 275, 255
 Turner, M. J. L., et al. 2001, *A&A*, 365, L27
 Yakovlev, D. G., & Pethick, C. J. 2004, *ARA&A*, in press (astro-ph/0402143)
 Zavlin, V. E., & Pavlov, G. G. 2002, in *Proc. 270 WE-Heraeus Seminar on Neutron Stars, Pulsars, and Supernova Remnants*, ed. W. Becker, H. Lesch, & J. Trümper (MPE Rep. 278; Garching: MPE), 263